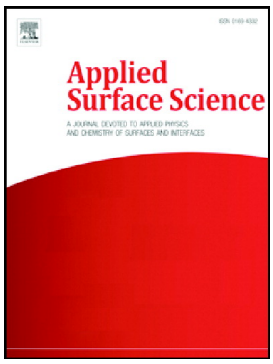

A density functional theory analysis on syngas adsorption on NiO (100) surface

Yue Yuan, Xiuqin Dong, Luis Ricardez-Sandoval

PII: S0169-4332(19)32598-X

DOI: https://doi.org/10.1016/j.apsusc.2019.143782

Reference: APSUSC 143782

To appear in: *Applied Surface Science*

Received date: 14 April 2019

Revised date: 16 August 2019

Accepted date: 23 August 2019

Please cite this article as: Y. Yuan, X. Dong and L. Ricardez-Sandoval, A density functional theory analysis on syngas adsorption on NiO (100) surface, *Applied Surface Science*(2019), https://doi.org/10.1016/j.apsusc.2019.143782

A Density Functional Theory Analysis on Syngas Adsorption on NiO (100) surface

Yue Yuan[1,2], Xiuqin Dong[1], Luis Ricardez-Sandoval[2*]

[1] Chemical Engineering Department, Tianjin University, No. 92 Weijin Rd, Tianjin 300072, China

[2] Chemical Engineering Department, University of Waterloo, 200 University Ave W, Waterloo, ON N2L 3G1, Canada

Abstract

Oxygen carrier (OC) design can effectively improve the performance of chemical looping combustion (CLC) and realize fossil fuel combustion at low energy-cost CO_2 capture. This study describes the adsorption principles of syngas (i.e. CO and H_2) on a clean Nickel Oxide (100) surface under single and multiple nearest neighbor effects. The results show that the adsorption stability of CO and H_2 is mostly weakened by the first neighbor compared to rest. With the same species as nearest neighbors (uniform adsorption), syngas adsorption stability is reduced when the number of neighbors increases. Similarly, when compared to uniform adsorption, the adsorption stability of CO and H_2 is slightly stronger with neighboring sites occupied with different species (hybrid adsorption). In addition, a lower degree of symmetry tends to strengthen CO and H_2 adsorption. Results from this analysis show that the adsorption stability of CO and H_2 with neighbors are highly related to steric, hybrid and symmetry effects. An electronic property analysis was performed to further support the key role of hybrid neighboring effects in the adsorption process of syngas on the Nickel Oxide (100) surface.

Keywords: Oxygen carrier, syngas, neighboring hybrid adsorption effect, adsorption stability.

Correspondence concerning this article should be addressed to Luis Ricardez-Sandoval at laricard@uwaterloo.ca.

1. Introduction

Fossil fuel combustion is the primary resource for power generation in the world. [1] Due to greenhouse gases effects, CO_2 emissions coming from fossil fuel combustion have risen major environmental concerns such as global warming. [2, 3] Hence, the development of highly efficient power generation systems that can mitigate CO_2 emissions are in critical need. The current technologies that have been considered for CO_2 capture include pre-combustion, post-combustion and oxy-combustion. The common factor in these technologies is the high energy consumption costs that are required to operate the major units in those processes and therefore diminishes the efficiency of the fossil-fired power systems. [4, 5] Chemical looping combustion (CLC) is a reduction-oxidation (redox) process that has been recently considered as a suitable CO_2 capture alternative due to its potential ability to avoid energy-intensive gas-gas separation processes. [6] CLC has attracted much attention since it involves an *in-situ* CO_2 separation property, i.e. direct contact of fuel and air is avoided thus producing an almost pure CO_2 stream. [7] The inherent separation of CO_2 in CLC minimizes the energy cost for CO_2 capture, which makes this process economically attractive. For instance, compared to the traditional pulverized fuel-fired power plant, CLC process only has an increment of 12-22% of energy; [8-10] most of this energy is being used to dispose the CO_2 captured from this technology (not for the actual CO_2 separation). One key player in CLC is the oxygen carrier (OC) material, which acts as a chemical intermediate to transfer oxygen within the CLC process. Analyzing the behavior of OC during operation is a key consideration for the process since they will significantly impact CLC performance [11, 12] and the design and operation of CLC reactors, e.g. the bed material and solid circulation rates. [10-13] Current OC materials often considered are metal oxides such as NiO, [14] Fe_2O_3 [15] and CuO. [16] Due to its favorable kinetics and potential catalytic abilities to break C-C and C-H bonds, NiO is one of the most widely used OC materials. Though Ni-based OCs are facing key obstacles such as cost and toxicity, they still attract much attention due to its high performance under harsh operating conditions. [17] The first step of the redox reaction of NiO with fuel molecules is adsorption. This phenomenon will affect the

electronic properties of both, the surface of OC materials and the nearby (neighbor) adsorbed molecules. The effect of the neighboring adsorbed molecules is relevant, particularly for adsorption studies on catalytic materials since they may change the structural configuration of the catalytic surface. In the modification of semiconductor surfaces, Ren et al. [18] have shown that the neighboring adsorbed H could induce the production of the ferromagnetic order of Si dangling bonds, which provides a way to promote magnetism on the Si (111) surface. It has been shown that neighboring effects also play a key role in the decoration of polymers. The neighboring linkers decorated on the adsorbents benefit the adsorption of specific molecules, [19] which could significantly increase the saturated adsorption capacity. Hence, neighboring effects impacts both the adsorbed molecules and the decorated surface. Furthermore, the surface decorated functional groups, which can be seen as the neighboring adsorbed molecules, also affect the surface adsorption as well as the elementary reactions. [20, 21] The different adsorption kinetics in consideration of the neighboring adsorption effects will enhance or constrain the subsequent surface reactions by determining the surface site occupation by the fuel molecules.

Although several OC materials have been screened for the CLC process, most of those studies have been conducted in experimental laboratories. [22, 23] Computational research studies in this emerging CO_2 capture area are still quite limited. To the authors' knowledge, a study on the adsorption principles of the fuel molecules on OC materials is not currently available in the open literature. Therefore, the atomistic and molecular behavior of OCs is unclear even for the most studied OC materials such as NiO. Density functional theory (DFT) can be an efficient means to explore the behavior of elemental reaction systems and provide insight into the expected events that are likely to occur in those systems. [24-26] Although there is a limited amount of reports on OC behavior using DFT, no theoretical report of the neighboring effects on OC surface has been established. The nearest neighbors can dramatically affect the heterogeneous reactions since they can modify the adsorption behavior, or even the surface electronic structure [27, 28], thus making the

neighboring effects non-negligible. Studies on this topic will be instrumental in providing insights on the OC performance in the design and operation of the CLC process.

This study presents an analysis of the neighboring effects on NiO with syngas, i.e., CO and H_2. In this work, the possible environments of the loading fuel syngas molecules are considered to provide a systematic adsorption study for this process. The adsorption energy as well as the electronic properties of the NiO surface have been analyzed and reported in this work. Through this study, the neighboring effects of the studied system are given to guide the expected subsequent reactions that may occur in this system and provide a useful reference for the design of a micro-kinetic model for this process.

This study is organized as follows: the computational model and theoretical methods used in this study are described in section 2. The structural properties and adsorption energy are listed and compared in section 3. Comparisons showing the neighboring effects, especially those pertaining to hybrid adsorption effects (i.e. those involving adsorbed molecules of different species) are discussed in this section. An electronic property analysis on the adsorption properties of syngas on the NiO surface is presented at the end of section 3. Concluding remarks are presented at the end of this study.

2. Computational Model and Methodology

First-principles simulations have been conducted with the Vienna Ab Initio Simulation Package (VASP). The Projector-augmented Wave (PAW)[29, 30] method with the Generalized Gradient Approximation(GGA) of Perdew-Burke-Ernzerhof has been used in this work to describe the wave-functions of the atomic cores system[31]. The energy cut-off of 400 eV was considered; moreover, a Gamma-centered mesh of 2×2×1 was established for the NiO surface calculations with a converge criteria of 1×10^{-5} eV by calculated energy, which provides sufficient accuracy in the calculations[32].

The conventional Local Density Approximation (LDA) and GGA cannot be applied to

the treatment of the electronic structure of the elements studied in this work since some of the ions contain partly filled *d* or *f* shells[33]. Therefore, the GGA with the unrestricted Hartree-Fock (UHF) approach (GGA+U) was employed to conduct accurate calculations of the surface properties. With the Hubbard U term, the electrons can be properly localized in the states and the U term works as the onsite Coulombic interactions between 3d electrons[34]. In this study, U =6.3 eV and J=1.0 eV were used to predict the properties of the system[35]. The calculated lattice constants for NiO are a=b=c=4.161 Å and α=β=ɣ=90°, which are consistent with reported experimental results (i.e., a=b=c=4.15 Å and α=β=ɣ=90°) [36]**.** The prediction of the bulk NiO property using the selected modification parameters U and J has been shown to be accurate when compared with experimental reports. In addition to the simulated NiO lattice constants obtained in this report, the system description of NiO surface such as adsorption behavior could be accurately predicted with the same Hubbard-U correction parameters employed in this study according to previous reports [35, 37, 38].

A 6-layer nickel oxide slab model has been constructed with the bottom four layers fixed to simulate syngas on the NiO surface. This slab model configuration has been shown to provide sufficiently accurate results.[39] The NiO bulk structure was obtained from the Inorganic Crystal Structure Database (ICSD) provided by FIZ Karlsruhe with the database code ICSD 182948 and proposed by Yang *et al* [30]. The crystal structure of NiO is the same as that of NaCl, which is a face-centered cubic (fcc) lattice structure for Ni^{2+} and O^{2-}. Each nickel ion is surrounded by six oxygen ions with an octahedral symmetry[40]. Since the nonpolar plane NiO (100) has been proven to be the most stable surface, a cleaved surface of NiO (100) with a 15 Å vacuum gap is used in this study to perform the adsorption calculations[41, 42]. Carbon monoxide has only one carbon-oxygen bond which is about 1.14362 Å long while the H_2 molecule also has only one hydrogen-hydrogen bond of 0.75117 Å. The adsorption geometry of CO is at the top of the Ni atom with the C-O bond located vertically with respect to the NiO surface. This configuration is the most stable

geometry with the minimum energy[43]. The further reaction of CO with NiO is that the C atom in CO scavenges the O on NiO surface, which makes the vertical CO (with C close to the surface) a more reasonable geometry for further reactions. As for H_2 molecule, the selected geometry is also at the top of Ni due to the tendency of H_2 breaking at the top of Ni[44] and the linear molecule H_2 also keeps vertical with the surface from the aspect of stability and small steric effect. The optimized adsorption configurations are provided as supporting information.

The adsorption energy of CO on NiO surface is calculated as follows:

$$\Delta E_{adsorption} = E_{system} - E_{freefuel} - E_{surface}$$

where E_{system} is the overall energy of the system with the reacted CO or H_2 molecules, $E_{freefuel}$ refers to the energy of the free fuel molecule (i.e. CO or H_2) whereas $E_{surface}$ represents the energy of the OC surface (NiO).

3. Results and discussion

This section presents the results obtained from this study. The sites considered on the NiO surface and the notation adopted for the adsorption geometries are presented first. The structural properties from the adsorption of syngas (i.e. CO and H_2) on the NiO surface are presented next. The adsorption principles of CO and H_2 obtained according to the adsorption energy analysis with uniform neighboring molecules, i.e., molecules of the same species, and the hybrid adsorption effects caused by the geometry containing different molecules at the nearest neighboring sites are presented thereafter. An analysis of the projected density of states, which supports the primary outcomes of this study at the electronic scale, are provided at the end of this section.

3.1 Structure characterization

Figure 1 presents the NiO structure model used in the present study. As shown in this figure, four closest neighboring sites are considered in this study to reveal the tendencies of the neighboring effects on which the oxidation of CO and breaking of H_2 to form H_2O are expected to occur. The four sites selected have the closest distances with the adsorption site labeled as 0 in the figure and which is expected to have the strongest interactions with the adsorbed CO or H_2 neighbors located in

positions 1, 2, 3 and 4 in the figure. To distinguish between the different adsorption geometries, the following notation is established from heretofore: C and H stand for CO and H_2 occupied sites on the NiO surface, respectively; * stands for an empty site. When naming a particular geometry, the order follows the site numbering indicated in Figure 1; the 5^{th} position in the name suggests the 0^{th} site. For example, the geometry HHHHH indicates the study of H_2 adsorption at the 0^{th} site with 4 H_2 nearest neighboring sites. If site 1 and 3 are empty and site 2 and 4 are occupied by CO and H_2, respectively, then that geometry will be referred to as *C*HC or *C*HH depending on whether CO or H_2 adsorption is considered at the 0^{th} site.

3.2 Structural property analysis

Three types of symmetries have been considered in the present system. As shown in Figure 2(a), symmetry 1 represents a line symmetry with only one axis of symmetry. As for symmetry 2, (Figure 2(b)), there are two axes of symmetry, which is also a point symmetry structure. Moreover, symmetry 3 has the highest degree of symmetry which has four axes of symmetry (Figure 2(c)).

Tables 1 and 2 present the distances between the CO and H_2 molecules and the adsorbed Ni site on the NiO surface, respectively. As mentioned above, uniform adsorption is used here to refer to the adsorption of CO (H_2) with the same molecules of CO (H_2) already adsorbed at the neighboring sites while hybrid adsorption indicates CO or H_2 adsorption with the different molecules of H_2 or CO captured at the closest neighboring sites.

As shown in Table 1, the distance between the adsorbed species and the adsorbed site increases from ****C to C***C which suggests that the adsorbed CO molecule would be repelled by the neighboring attached CO molecule. However, when the neighboring site is occupied by H_2 (i.e., H***C), the repulsion effect is much smaller than that obtained from the neighboring effect of CO. This change in behavior is due to the steric effects, which are more significant for CO than for H_2. Note that the distance between the carbon atom of adsorbed CO and its connected Ni on NiO (100) is reported to be 2.07 Å [45]. The calculated distance between the carbon of CO and its connected Ni in

this manuscript is 2.076 Å at low coverage. Thus, there is consistency between the experimental data and the present DFT calculations, which further validates the results obtained in this work. Both carbon and oxygen atoms in the CO molecule have relatively larger van der Waal radius (1.885 Å and 1.514 Å) compared to that of H atom (1.394 Å) in H_2; hence, higher steric repulsions are expected by the former species. [46] The results shown in Table 1 for CC**C and CCC*C indicate that, when the structures belong to the same symmetry (symmetry 1), the repelling effects are more notable as the number of nearest neighbors increases. This behavior was also observed for the hybrid adsorption of CO (i.e., between HH**C and HHH*C). As for symmetry 2, the distance from C*C*C (2.043 Å) increases when the empty sites are replaced with two H_2 neighbors (CHCHC, 2.058 Å). As shown in Table 1, the distance in the highest degree of symmetry (i.e. CCCCC) is smaller than that observed for ****C. This observation may be expected since the linear CO molecule tends to tilt to weaken the steric effect between the neighbors and the adsorbed molecule while the tilting in a highly symmetric geometry is very unlikely to happen. Also, a comparison between the distances obtained for CC**C (symmetry 1), C*C*C (symmetry 2) and CCCCC (symmetry 3) tend to suggest that a high degree of symmetry of a uniform CO adsorption may lead to shorter distances even when the number of nearest neighbors is higher. On the other hand, the hybrid adsorption geometries of CO with H_2 occupied sites did not present the same behavior, i.e., the distance predicted for HH**C (symmetry 1) is smaller than that obtained for H*H*C (symmetry 2); similarly, the distance of HHHHC (symmetry 3) is larger than that of ****C (i.e., no neighboring sites), as shown in Table 1. Consequently, the neighboring effects of hybrid CO adsorption with H_2 as neighboring sites would not be affected by the degree of symmetry as much as that observed from the uniform CO occupied sites. Nevertheless, H_2 nearest neighbors present shorter distances compared to CO nearest neighbors with the same number of neighboring molecules; except for the case of four (full) nearest neighbors HHHHC and H*H*C at symmetry 2, which present larger distances than that of CCCCC and C*C*C. As mentioned above, this is caused by the stronger symmetry

effects of the neighboring CO molecule. These results suggest that a high coverage NiO surface will not enhance CO adsorption due to low availability of active NiO sites and the high degree of symmetry. The neighboring attached CO molecules lead to the more substantial repelling effect rather than the neighboring attached H_2. These observations have been corroborated by an adsorption energy analysis that is presented in the next section.

Table 2 presents the structural properties of H_2 adsorption as a function of both the number and type of nearest neighbors. As shown in Table 2, a similar trend to that observed for CO adsorption is also observed for H_2 adsorption. An increase in the number of H_2 nearest neighbors results in stronger repelling effects with the same degree of symmetry (symmetry 1) whereas a high degree of symmetry for H_2 adsorption with H_2 neighboring sites makes the tilting of the linear H_2 molecule very unlikely thus producing a structure with shorter distances between the adsorbed H_2 molecule and the surface. Regarding symmetry 2 configurations for H_2, the distance in CHCHH (2.498 Å) is larger than that in C*C*H (2.492 Å) due to the increasing number of the neighbors. As shown in Table 2, the same number of CO occupied neighboring sites often results in more significant repelling effects than those observed for H_2 occupied neighboring sites, except for the case of CCCCH. The distance of CCCCH is smaller than that of HHHHH which is mostly due to the stronger symmetry effect observed for CO neighboring molecules than that of H_2. A higher-coverage NiO surface tends to repel the H_2 from the surface due to the steric effects and the higher degree of symmetry. The attached CO neighbors will lead to a more significant repelling effect rather than having H_2 as nearest neighbors.

3.3 Adsorption energy analysis

To assess the energetic adsorption effects of syngas (CO and H_2) on the NiO (100) surface, the adsorption of CO and H_2 with the same (uniform) neighboring molecules was analyzed first. The adsorption energy can be regarded as the isothermal enthalpy change of adsorption in the system; this energy is often found to be negative, which indicates that the adsorption process is both exothermic and spontaneous. A large

absolute value of the negative adsorption energy is an indication of large amounts of heat generated from the adsorption process. Thus, a release of heat (energy) is often observed during the adsorption process. Figure 3 shows the adsorption energy of CO with and without CO nearest neighbors (uniform adsorption). According to DFT analysis of CO adsorption on NiO, CO adsorbed on a clean NiO surface releases about 1.5618 eV of heat. With one nearest neighboring molecule of CO (3.194 Å), the adsorption energy of CO changes into -0.2803 eV, which represents 18% of the total heat generated on the clean surface without CO neighboring molecules. Note that the estimated adsorption energy (0.28 eV) agrees with the experimental result in the low-coverage regime (0.3 eV) [47]. With two or three neighboring molecules of CO, the changes in the adsorption energy are less than 10% respecting that with no neighbors. These results indicate that the first adsorbate molecule on the NiO surface significantly weakens the adsorption of the same molecule on a nearby site. As for the geometry with four nearest neighbors, the adsorption energy changes to +0.0622 eV. Hence, the CO adsorption with four nearest neighbors can hardly happen due to the endothermic process as indicated from the positive enthalpy change. To further support this analysis, the CO adsorption with five neighboring occupied molecules was conducted and resulted in adsorption energy of + 0.0339 eV. The 5^{th} neighboring site is the 2^{nd} closest Ni to the adsorption site which has a distance of 4.1696 Å from the adsorption site. The similar behavior was observed for the H_2 adsorption on NiO with H_2 neighboring molecules (uniform adsorption), as shown in Figure 3. The difference in adsorption energies decreases and flattens out with the 3^{rd} and 4^{th} loading molecules, respectively. Particularly for the H_2 loading with four nearest neighbors, the adsorption energy is the lowest due to its fully occupied neighboring sites, which is still negative and indicates greater stability of the H_2 adsorption compared to that of the CO adsorption with 4 CO neighbors. The adsorption energy analysis of uniform adsorption suggests that the NiO surface with high coverage of uniform neighbors tends to be unreactive to adsorb CO and H_2.

Figure 4(a) presents a comparison between CO uniform adsorption and CO hybrid

adsorption as a function of the number of nearest neighbors. Uniform adsorption energy with the same number of neighbors are also presented in this figure for comparison purposes.. The neighboring occupied geometry sharing the same x value means that they have the same number of occupied neighboring molecules as well as the same degree of symmetry. Hybrid adsorption distinguishes from the uniform adsorption by the different neighboring occupied molecules with the studied adsorption molecule. For example, the CO hybrid adsorption considers the neighboring sites occupied by H_2 while the H_2 hybrid adsorption estimates the neighboring sites employed by CO. As shown in Figure 4(a), the difference in adsorption energies between the uniform adsorption and hybrid adsorption increases as the number of nearest neighbors increases. The degree of symmetry increases from none symmetry (C***C and H***C) to symmetry 3 (CCCCC and HHHHC) with the increasing number of neighbors. As discussed in the previous section, a higher degree of symmetry will lead to weaker adsorption stability for both CO and H_2 adsorption, which is shown in figure 5 and discussed at the end of this section. The results from Figure 4(a) shows that this effect is more significant on CO occupied neighboring geometry since it contributes to more considerable differences in adsorption energy between CO adsorption with CO neighbors than on CO adsorption with H_2 neighbors. As a result, it is expected that the stability of CO adsorption with H_2 neighboring molecules is relatively higher when compared to uniform CO adsorption. Figure 4(a) also shows that the difference in energy between CCCCC and HHHHC (symmetry 3) is much more significant than that between C***C and H***C (no symmetry). The less reduced stability observed with hybrid nearest neighbors species compared to that with uniform adsorption may be due to the different electronic structures of the adsorbed molecule (CO) and the Ni on the surface (see section 3.4).

Figure 4(b) compares the energetic results for hybrid and uniform H_2 adsorption. As shown in this figure, H_2 adsorption is more stable with one H_2 nearest neighbor rather than with one CO nearest neighbor. This may be due to the much smaller effect of one H_2 molecule on the surface compared to that of CO as a neighbor (see section 3.4).

When the number of the neighboring occupied sites increases (HH**H and HHH*H), the H_2 uniform adsorption is weaker than the hybrid adsorption due to the magnified neighboring H_2 effects, as shown in Figure 4(b). As mentioned in section 3.2, CO as neighbor leads to a more significant steric effect than H_2 does. Thus, the stability of H_2 adsorption is more negatively affected by the steric repulsions with hybrid CO neighbors rather than that with uniform H_2 neighbors. As mentioned above, a high degree of symmetry has a more profound effect on the CO occupied geometry. As shown in Figure 4(b), the stronger steric and symmetry effects caused by the presence of four CO neighbors in H_2 adsorption lead to a significant decrease in adsorption energy. From Figure 4, the hybrid effect weakens the negative impact of the neighbors on both CO and H_2 adsorption. Particularly, the adsorption energy of H_2 on a perfect NiO (100) surface obtained from experimental data tends to be low, i.e., smaller than 0.22 eV as reported in a previous study [48]. The computed adsorption energy of H_2 in this study with low coverage is about 0.1 eV, which tends to agree with that experimental observation.

Figure 5 shows the CO and H_2 adsorption with four nearest neighbors using molecules of different species whereas their location is given by the notation described in section 3.1. CO adsorption is an exothermic process, thus generating a negative value of adsorption energy. A higher absolute value of adsorption energy indicates higher adsorption stability. According to Figure 5(a), an increase in the number of H_2 nearest neighbors leads to stronger CO adsorption (i.e. higher absolute value of adsorption energy). As shown in Figure 5(a), a higher degree of symmetry (symmetry 2 higher than symmetry 1) weakens the CO adsorption. As for H_2 adsorption (Figure 5(b)), this is affected by both hybrid and steric effects. Therefore, the heat generated from H_2 adsorption first increases caused by the attached CO included in the nearest neighbors(shown as CHHHH), which highlights the hybrid effect on H_2 capture, and then it tends to decrease since the CO steric effect dominates the process. Furthermore, Figure 5(b) also shows that adsorption stability is negatively affected when there exists higher degrees of symmetry. By comparing the

adsorption energy between CHCHH (symmetry 2) and CCHHH (symmetry 1), it can be concluded that a higher degree of symmetry will reduce the heat generated from H_2 adsorption, which indicates weaker adsorption stability. This same behaviour was also observed for CO adsorption.

3.4 Electron property analysis

The electronic properties of CO and H_2 uniform and hybrid adsorption have been analyzed to provide further insight into the neighboring effects of these species on the NiO surface. Figure 6 presents the molecular orbitals of CO and Ni 3d orbitals, which provides a comparison between the free gas with NiO surface system and the adsorbed system. According to Figure 6(a), 2π* and 5σ orbitals of CO and 3d orbitals of Ni have similar energy levels. Note that 1π orbital of CO mainly contributes to the bonding between C and O in CO molecule[49]. Therefore, CO as an adsorbate primarily interacts with Ni by hybridization between 5σ and 2π* orbitals of CO and 3d orbitals of Ni on the surface. This conclusion agrees with previous reports of CO adsorption [50, 51]. Figure 6(b) shows that CO adsorption leads to the spreading of the d orbitals of Ni. A small peak of Ni 3d orbital appears at the same energy level as the 2π* orbital of CO. The electron occupation at 5σ orbital of CO dramatically decreases and shifts to a lower energy level due to the 5σ-d forward donation effect[52]. According to the comparison between the non-adsorbed system and the adsorbed system, as shown in figure 6(c) and 6(d), the 3d orbitals of Ni shift to a lower energy level and the molecular orbitals of CO shift in the same direction, which indicate a more stable system upon adsorption. The changes of 5σ and 2π* orbitals shown in Figure 6(d) result from the 5σ-d forward donation and d-2π* back-donation [49, 52, 53].

Figure 7 provides a comparison between the free H_2 on NiO surface system and the adsorbed system to study the interactions between the H_2 molecular orbitals and the 3d orbitals of the transition metal Ni. Figure 7(a) shows that 3d orbitals of Ni have energy level overlapped with bonding σ orbital and antibonding σ* orbital of H_2. The interaction between the H_2 and surface Ni mainly results from the interactions between 3d orbitals and σ molecular orbital. H_2 adsorption leads to the spreading of

σ* orbital. According to Figure 7(c), no apparent change appears for 3d Ni orbitals except for the slightly spreading at the energy level of σ* orbital. The H_2 adsorption barely affects the surface electronic structure. Compared to CO adsorption, H_2 has a weaker effect on the surface as an adsorbate. Therefore, stronger adsorption of CO compared to that of H_2 is expected. This also explains why the absolute value of the CO adsorption energy is much larger than that of H_2 adsorption, as shown in Figure 3. As for the molecular orbitals of H_2, the peak of σ orbital shifts to a lower energy level due to the interaction between the surface Ni and H_2, thus increasing the stability of the system.

By comparing Figure 6(c) and Figure 7(c), the 3d orbitals of Ni are apparently affected to a larger extent by CO adsorbate compared to H_2. A weaker interaction between H_2 and surface Ni suggests that it may be more favorable for H_2 to migrate from the Ni site to its neighbor for further reactions. The weaker interaction is also corroborated by the lower adsorption energy of H_2 compared to that of CO, as discussed in section 3.3. Furthermore, Figure 6(d) presents a slight decrease of the 2π* orbital (antibonding orbital) resulted from CO adsorption while Figure 7(d) shows a modest increase of the σ* orbital (antibonding orbital) caused by H_2 adsorption. More packed antibonding orbital of H_2 suggests a weaker H_2 inner bond. Therefore, a higher reaction activity towards breaking the inner band of H_2 compared to CO can be anticipated.

Figures 6 and 7 provide the interactions between the adsorbates and studied surface. Based on a previous analysis, the neighboring effect of CO and H_2 on the studied surface and adsorbates are shown in figure 8. To emphasize the neighboring effect, the extreme conditions are considered for both CO and H_2 adsorption as where the four nearest neighbor sites are fully occupied. With four nearest CO neighbors, the d orbitals of Ni at HOMO orbital broadens and its left edge shifts to a lower energy level in Figure 8(a) while no significant change appears for the d orbitals of Ni with 4 H_2 neighbors. Accordingly, the closest active site of Ni is more significantly affected by the neighboring CO than by the neighboring H_2. The change in the molecular

orbital shown in figure 8(b) gives the same trend as mentioned above. The CO neighbors significantly influence the molecular orbitals of the adsorbed CO while H_2 neighbors only lead to a slight shift to a higher energy level. This explains the more significant repelling effect on the adsorbed species coming from the CO neighbors to H_2 neighbors. This result agrees with the conclusions obtained from the adsorption energy in Figure 4(a). Hence, a clean NiO surface is more likely to attract CO molecules rather than a surface with high coverage. The peak at $2\pi^*$ antibonding orbital splits into two new peaks. The bonding between C and O in CO molecule appears to change by the CO neighboring effect. As shown in Figure 8(c), the electron density occupancy of 3d orbitals of Ni with 4 CO neighbors spreads to a lower energy level while it almost remains constant with 4 H_2 neighbors. The fully occupied CO neighboring configuration leads to an apparent broadening of the σ orbital of adsorbed H_2 compared to that resulted from a fully occupied H_2 neighbor configuration. The mentioned change also comes from the more substantial repelling effect caused by the CO neighbors. The aforementioned results corroborate the conclusions obtained from Figure 4(b). Comparing Figure 8(a) and Figure 8(c), the change in the electronic structure of H_2 adsorbed surface stemming from neighboring effect is not as apparent as that of H_2 adsorbed surface. This is due to the smaller difference in H_2 adsorption energy compared to that in CO, which is also reflected by the results presented in Figure 3.

Figure 9 compares the CO adsorption in CCHH and CHCH (symmetry2 compared to symmetry1) neighboring configurations to emphasize the symmetry effect shown from the electron distribution. For CO adsorption in Figure 9(a), the 3d orbitals of Ni at low energy levels are slightly more packed and tend to spread in CCHHC compared to that in CCHHC. As shown in Figure 9(b), bonding orbitals of CO in CHCHC (symmetry 2) broaden and experience a small shift compared to that in CCHHC (symmetry 1). Therefore, a higher energy level of CHCHC system is expected as well as lower system stability. In particular, the antibonding orbital $2\pi^*$ in CHCHC (symmetry 2) is more packed, thus weakening the bond of C and O in CO molecules.

According to Figure 9(c) and Figure 9(d), H_2 adsorption in a system with a higher symmetry degree (CHCHH, symmetry2) leads to similar spreading on 3d orbital of Ni, σ and σ* orbitals of H_2. More packed antibonding σ* orbital of H_2 demonstrates the weakened inner bond of H_2. The geometry with a higher degree of symmetry (i.e., CHCHC and CHCHH) lowers the stability of the adsorption while structures that present a lower degree of symmetry (i.e., CCHHC and CCHHH) for both CO and H_2 adsorbed molecules do not show that effect. This result agrees with the findings presented in Figure 5, i.e., a higher degree of symmetry (symmetry 2 compared to symmetry 1) generates less adsorption heat.

Figure 10 presents the electronic property analysis for the hybrid adsorption effects. Figure 10(a) and Figure 10(b) show a larger spreading in both Ni 3d orbital and CO molecular orbitals in CCHHC (with hybrid neighbors) system compared to that in CCCCC (without hybrid neighbors) system. Stronger interaction between CO and the surface is predicted. Figure 10(c) and Figure 10(d) reveal the similar broadening trend of Ni 3d orbital and H_2 molecular orbitals via the comparison between CCHHH (with hybrid neighbors) and HHHHH (without hybrid neighbors). This result indicates that hybrid effects will reduce the negative effect on both CO adsorption and H_2 adsorption caused by neighbors, which agrees with the adsorption energy analysis presented in Figures 4 and 5.

Conclusions

This study provided new insights into the adsorption of syngas (i.e., CO and H_2) in the NiO surface affected by the surrounding surface environment. According to the structural property analysis, the adsorption sites tend to repel the attached CO or H_2 away with an increasing number of neighbors. This is an indication of the steric effects on the surface, which may become more significant for nonlinear molecules like methane. A CO neighbor leads to a larger distance between the adsorption site and the attached molecule compared to the neighbor of H_2. For both CO and H_2 adsorption, the most significant decrease of the adsorption energy is observed with

one nearest neighbor. This suggests that after the first neighboring molecule has been attached on the surface, the adsorption stability does not tend to change significantly as the number of the neighboring adsorbed molecules increases. The energetic analysis shows that the hybrid adsorbed sites lead to less negative effects on CO and H_2 adsorption caused by neighbors while the steric effects should be considered when CO is the neighboring molecule. A higher degree of symmetry leaves the adsorption molecule no tilting space which leads to weakening adsorption stability. This study indicates that the adsorption strength is a combination of the hybrid effect, the space limit and the symmetry effects. Electronic property analysis on the different configurations was performed to validate the insights gained through this study. Insights from this work will be essential to develop highly predictive microkinetic models for syngas on OC materials thus promoting the development of CLC technology.

Acknowledgments

The authors gratefully acknowledge the support provided by the Chinese Scholarship Council and Sharcnet to develop this research. This work was made possible by access to the facilities of the Shared Hierarchical Academic Research Computing Network (SHARCNET: www.sharcnet.ca) and Compute/Calcul Canada.

References

[1] F. Birol, Key world energy statistics, in: International Energy Agency, 2017.
[2] K. Jeong, T. Hong, J. Kim, Development of a CO_2 emission benchmark for achieving the national CO_2 emission reduction target by 2030, Energy and Buildings, 158 (2018) 86-94.
[3] K. Zickfeld, A.H. MacDougall, H.D. Matthews, On the proportionality between global temperature change and cumulative CO2emissions during periods of net negative CO_2 emissions, Environmental Research Letters, 11 (2016) 055006.
[4] J.D. Figueroa, T. Fout, S. Plasynski, H. McIlvried, R.D. Srivastava, Advances in CO_2 capture technology-The U.S. Department of Energy's Carbon Sequestration Program, Int. J. Greenh. Gas Con., 2 (2008) 9-20.
[5] M.H. Sahraei, D. McCalden, R. Hughes, L. Ricardez-Sandoval, A survey on current advanced IGCC power plant technologies, sensors and control systems, Fuel, 137 (2014) 245-259.
[6] Y. Yuan, H. You, L. Ricardez-Sandoval, Recent advances on first-principles modeling for the design of materials in CO_2 capture technologies, Chinese Journal of Chemical Engineering, (2018).
[7] L. Zeng, Z. Cheng, J.A. Fan, L.-S. Fan, J. Gong, Metal oxide redox chemistry for chemical looping processes, Nature Reviews Chemistry, (2018) 1.
[8] J. Adanez, A. Abad, F. Garcia-Labiano, P. Gayan, L.F. de Diego, Progress in Chemical-Looping Combustion and Reforming technologies, Prog. Energy Combust. Sci., 38 (2012) 215-282.
[9] L.F. de Diego, F. García-Labiano, P. Gayán, J. Celaya, J.M. Palacios, J. Adánez, Operation of A 10 kWth Chemical-looping Combustor during 200 h with A CuO-Al_2O_3 Oxygen Carrier, Fuel, 86 (2007) 1036-1045.
[10] M.M. Hossain, K.E. Sedor, H.I. de Lasa, Co-Ni/Al_2O_3 Oxygen Carrier for Fluidized Bed Chemical-looping Combustion: Desorption Kinetics and Metal-support Interaction, Chem. Eng. Sci., 62 (2007) 5464-5472.
[11] L. Wang, Q. Li, W. Qin, Z.M. Zheng, X.B. Xiao, C.Q. Dong, Activity of Fe_2O_3 and its Effect on Co Oxidation in the Chemical Looping Combustion: An Theoretical Account, in: Adv. Mat. Res., Trans Tech Publ, 2013. 2040-2044.
[12] X. Cai, X. Wang, X. Guo, C.g. Zheng, Mechanism study of reaction between CO and NiO(001) surface during chemical-looping combustion: Role of oxygen, Chem. Eng. J., 244 (2014) 464-472.
[13] M.M. Hossain, H.I. de Lasa, Chemical-looping combustion (CLC) for inherent CO_2 separations—a review, Chemical Engineering Science, 63 (2008) 4433-4451.
[14] P. Cho, T. Mattisson, A. Lyngfelt, Comparison of iron-, nickel-, copper-and manganese-based oxygen carriers for chemical-looping combustion, Fuel, 83 (2004) 1215-1225.
[15] T. Mattisson, A. Lyngfelt, P. Cho, The use of iron oxide as an oxygen carrier in chemical-looping combustion of methane with inherent separation of CO_2, Fuel, 80 (2001) 1953-1962.
[16] M. Wang, J. Liu, J. Hu, F. Liu, O2-CO2 Mixed Gas Production Using a Zr-Doped Cu-Based Oxygen Carrier, Industrial and Engineering Chemistry Research, 54 (2015) 9805-9812.
[17] P. Gayán, F. Luis, F. García-Labiano, J. Adánez, A. Abad, C. Dueso, Effect of support

on reactivity and selectivity of Ni-based oxygen carriers for chemical-looping combustion, Fuel, 87 (2008) 2641-2650.
[18] X.Y. Ren, Niu, C. Y., Yi, S., Li, S., Cho, J. H., Hydrogen adsorption induced nanomagnetism at the Si(111)-(7 × 7) surface, Physical Review B, 98 (2018) 195424.
[19] S. Zhang, Y. Li, C. Shi, F. Guo, C. He, Z. Cao, J. Hu, C. Cui, H. Liu, Induced-fit adsorption of diol-based porous organic polymers for tetracycline removal, Chemosphere, 212 (2018) 937-945.
[20] J. Wang, M. Yang, D. Deng, S. Qiu, The adsorption of NO, NH_3, N_2 on carbon surface: a density functional theory study, Journal of molecular modeling, 23 (2017) 262.
[21] X. Huang, W. Chu, W. Sun, C. Jiang, Y. Feng, Y. Xue, Investigation of oxygen-containing group promotion effect on CO_2 - coal interaction by density functional theory, Applied Surface Science, 299 (2014) 162-169.
[22] Z. Cheng, L. Qin, J.A. Fan, L.-S. Fan, New insight into the development of oxygen carrier materials for chemical looping systems, Engineering, (2018).
[23] L. Qin, M. Guo, Y. Liu, Z. Cheng, J.A. Fan, L.-S. Fan, Enhanced methane conversion in chemical looping partial oxidation systems using a copper doping modification, Applied Catalysis B: Environmental, 235 (2018) 143-149.
[24] L.I. Bendavid, E.A. Carter, CO_2 Adsorption on Cu2O(111): A DFT+U and DFT-D Study, J. Phys. Chem. C, 117 (2013) 26048-26059.
[25] A.s.R. Botello-Mendez, S.M.M. Dubois, A.I. Lherbier, J.C. Charlier, Achievements of DFT for the investigation of graphene-related nanostructures, PMID: 24937509, 47 (2014) 3292-3300.
[26] E.F.V. Carvalho, A.N. Barauna, F.B.C. Machado, O. Roberto-Neto, DFT study for the reactions of H atoms with CH_3OH and C_2H_5OH, Int. J. Quantum Chem, 108 (2008) 2476-2485.
[27] Y. Gauthier, M. Schmid, S. Padovani, E. Lundgren, V. Bus, G. Kresse, J. Redinger, P. Varga, Adsorption sites and ligand effect for CO on an alloy surface: a direct view, Phys. Rev. Lett., 87 (2001) 036103.
[28] H. Wang, W.F. Schneider, Effects of coverage on the structures, energetics, and electronics of oxygen adsorption on RuO_2(110), J Chem Phys, 127 (2007) 064706.
[29] P.E. Blöchl, Projector augmented-wave method, Phys. Rev. B, 50 (1994) 17953.
[30] G. Kresse, D. Joubert, From ultrasoft pseudopotentials to the projector augmented-wave method, Phys. Rev. B, 59 (1999) 1758.
[31] J.P. Perdew, K. Burke, M. Ernzerhof, Generalized gradient approximation made simple, Phys. Rev. Lett., 77 (1996) 3865.
[32] X. Cai, X. Wang, X. Guo, C.-g. Zheng, Mechanism study of reaction between CO and NiO (0 0 1) surface during chemical-looping combustion: role of oxygen, Chem. Eng. J., 244 (2014) 464-472.
[33] S. Dudarev, G. Botton, S. Savrasov, C. Humphreys, A. Sutton, Electron-energy-loss spectra and the structural stability of nickel oxide: An LSDA+ U study, Phys. Rev. B, 57 (1998) 1505.
[34] L. Qin, Z. Cheng, J.A. Fan, D. Kopechek, D. Xu, N. Deshpande, L.-S. Fan, Nanostructure formation mechanism and ion diffusion in iron - titanium composite materials with chemical looping redox reactions, J. Mater. Chem. A, 3 (2015) 11302-11312.
[35] G. Peng, L.R. Merte, J. Knudsen, R.T. Vang, E. Lægsgaard, F. Besenbacher, M.

Mavrikakis, On the mechanism of low-temperature CO oxidation on Ni (111) and NiO (111) surfaces, J. Phys. Chem. C, 114 (2010) 21579-21584.
[36] M.-C. Yang, B. Xu, S. Meng, J.-H. Cheng, C.-J. Pan, B.-J. Hwang, Electronic, Structural and Electrochemical Properties of $LiNixCuyMn_{2-x-y}O_4$ (0< x< 0.5, 0< y< 0.5) High-Voltage Cathode Materials in Li-Ion Batteries, in: Meeting Abstracts, The Electrochemical Society, 2010. 1009-1009.
[37] A. Rohrbach, J. Hafner, Molecular adsorption of NO on NiO(100): DFT and DFT+Ucalculations, Physical Review B, 71 (2005).
[38] A.M. Ferrari, C. Pisani, F. Cinquini, L. Giordano, G. Pacchioni, Cationic and anionic vacancies on the NiO(100) surface: DFT+U and hybrid functional density functional theory calculations, J Chem Phys, 127 (2007) 174711.
[39] L. Qin, Z. Cheng, M. Guo, J.A. Fan, L.-S. Fan, Morphology evolution and nanostructure of chemical looping transition metal oxide materials upon redox processes, Acta Mater., 124 (2017) 568-578.
[40] T. Klüner, H.J. Freund, J. Freitag, V. Staemmler, Laser - induced desorption of NO from NiO (100): Ab initio calculations of potential surfaces for intermediate excited states, J. Chem. Phys., 104 (1996) 10030-10040.
[41] M. Yan, S. Chen, T. Mitchell, D. Gay, S. Vyas, R. Grimes, Atomistic studies of energies and structures of (hk0) surfaces in NiO, Philos. Mag. A, 72 (1995) 121-138.
[42] P. Tasker, D. Duffy, The structure and properties of the stepped surfaces of MgO and NiO, Surf. Sci., 137 (1984) 91-102.
[43] I. Mehdaoui, T. Klüner, Bonding of CO and NO to NiO (100): a strategy for obtaining accurate adsorption energies, J. Phys. Chem. A, 111 (2007) 13233-13237.
[44] P. Jayapal, M. Sundararajan, I.H. Hillier, N.A. Burton, How are the ready and unready states of nickel - iron hydrogenase activated by H_2 A density functional theory study, Phys. Chem. Chem. Phys., 8 (2006) 4086-4094.
[45] J.T. Hoeft, M. Kittel, M. Polcik, S. Bao, R.L. Toomes, J.H. Kang, D.P. Woodruff, M. Pascal, C.L. Lamont, Molecular adsorption bond lengths at metal oxide surfaces: failure of current theoretical methods, Phys. Rev. Lett., 87 (2001) 086101.
[46] J. Badenhoop, F. Weinhold, Natural steric analysis: Ab initio van der Waals radii of atoms and ions, J. Chem. Phys., 107 (1997) 5422-5432.
[47] R. Wichtendahl, M. Rodriguez-Rodrigo, U. Härtel, H. Kuhlenbeck, H.-J. Freund, TDS study of the bonding of CO and NO to vacuum-cleaved NiO (100), Surf. Sci., 423 (1999) 90-98.
[48] J.A. Rodriguez, J.C. Hanson, A.I. Frenkel, J.Y. Kim, M. Pérez, Experimental and theoretical studies on the reaction of H_2 with NiO: role of O vacancies and mechanism for oxide reduction, J. Am. Chem. Soc., 124 (2002) 346-354.
[49] S.S. Sung, R. Hoffmann, How carbon monoxide bonds to metal surfaces, J. Am. Chem. Soc., 107 (1985) 578-584.
[50] X. Shi, S.L. Bernasek, A. Selloni, Formation, Electronic Structure, and Defects of Ni Substituted Spinel Cobalt Oxide: a DFT+U Study, The Journal of Physical Chemistry C, 120 (2016) 14892-14898.
[51] D. Sun, X.-K. Gu, R. Ouyang, H.-Y. Su, Q. Fu, X. Bao, W.-X. Li, Theoretical Study of the Role of a Metal - Cation Ensemble at the Oxide - Metal Boundary on CO Oxidation,

The Journal of Physical Chemistry C, 116 (2012) 7491-7498.
[52] D.-M. Huang, D.-B. Cao, Y.-W. Li, H. Jiao, Density function theory study of CO adsorption on Fe_3O_4 (111) surface, J. Phys. Chem. B, 110 (2006) 13920-13925.
[53] X. Yu, X. Zhang, L. Jin, G. Feng, CO adsorption, oxidation and carbonate formation mechanisms on Fe_3O_4 surfaces, Phys Chem Chem Phys, 19 (2017) 17287-17299.

List of Tables and Figures

Table 1 Structural properties of CO adsorption on NiO

	Uniform Adsorption		Hybrid Adsorption	
Symmetry	Geometry name	Distance [a]/Å	Geometry name	Distance/Å
none	****C	2.058		
none	C***C	2.076	H***C	2.059
symmetry 1	CC**C	2.071	HH**C	2.056
symmetry 2	C*C*C	2.043	H*H*C	2.068
symmetry 1	CCC*C	2.091	HHH*C	2.076
symmetry 3	CCCCC	2.05	HHHHC	2.067

a distance between the H closer to the surface in H_2 and the closest Ni to the mentioned H on the surface.

Table 2 Structural properties of H_2 adsorption on NiO

	Uniform Adsorption		Hybrid Adsorption	
Symmetry	Geometry name	Distance [a]/Å	Geometry name	Distance/Å
none	****H	2.543		
none	H***H	2.759	C***H	2.959
symmetry 1	HH**H	2.519	CC**H	3.132
symmetry 2	H*H*H	2.491	C*C*H	2.492
symmetry 1	HHH*H	2.542	CCC*H	3.018
symmetry 3	HHHHH	2.501	CCCCH	2.499

a distance between the H closer to the surface in H_2 and the closest Ni to the mentioned H on the surface.

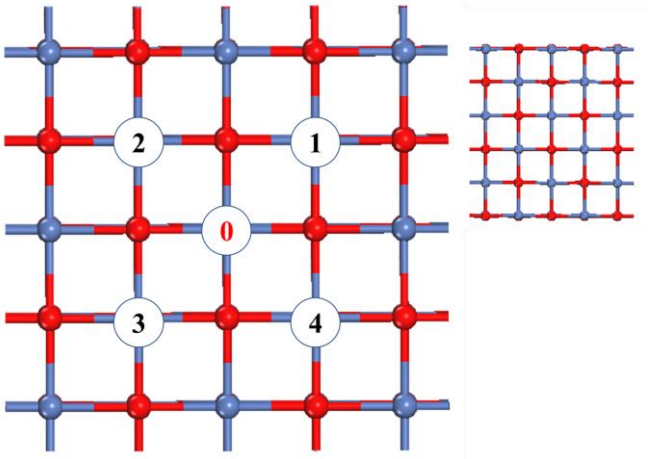

Fig. 1 Studied sites from 1 to 4, adsorption site labeled as 0

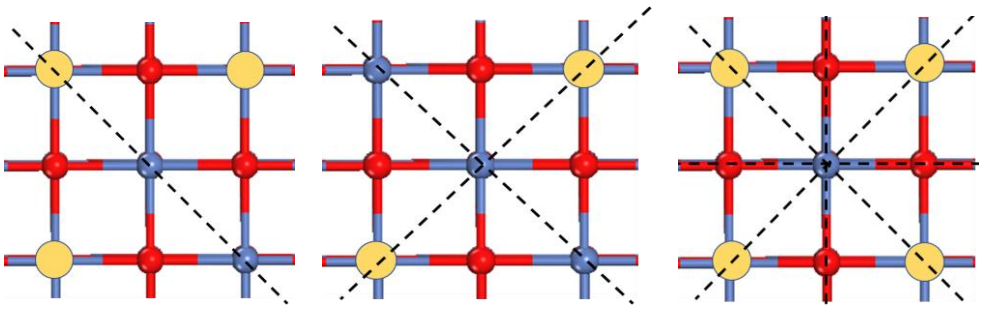

(a) **(b)** **(c)**

Fig. 2 Symmetry categories of the adsorption system, (a) symmetry 1, (b) symmetry 2 (c) symmetry 3

The yellow circles in the figure are the occupied sites on the surface.

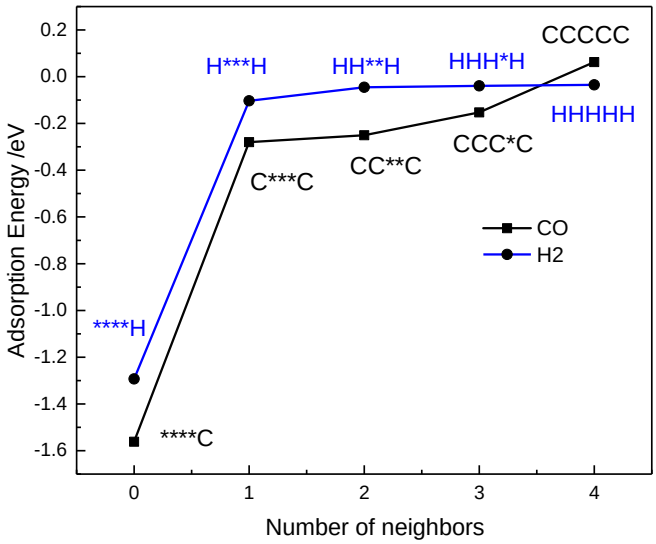

Fig 3. Adsorption energy of uniform loading molecules

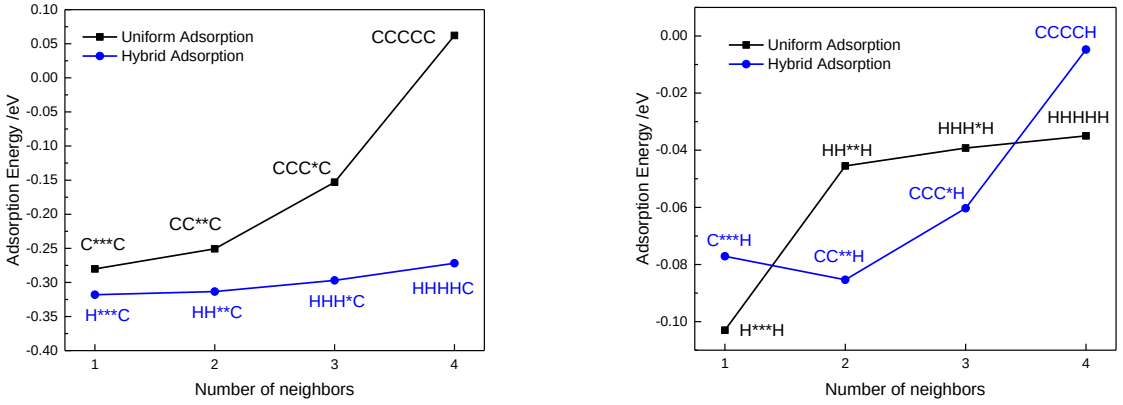

(a) **(b)**

Fig 4. (a) CO adsorption comparison and (b) H_2 adsorption comparison

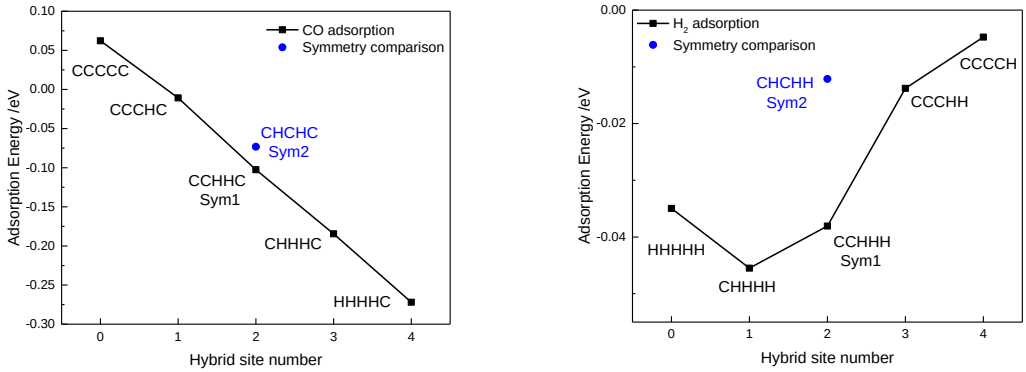

(a) **(b)**

Fig 5. Fully occupied nearest neighboring Site (a) CO adsorption and (b) H_2 adsorption

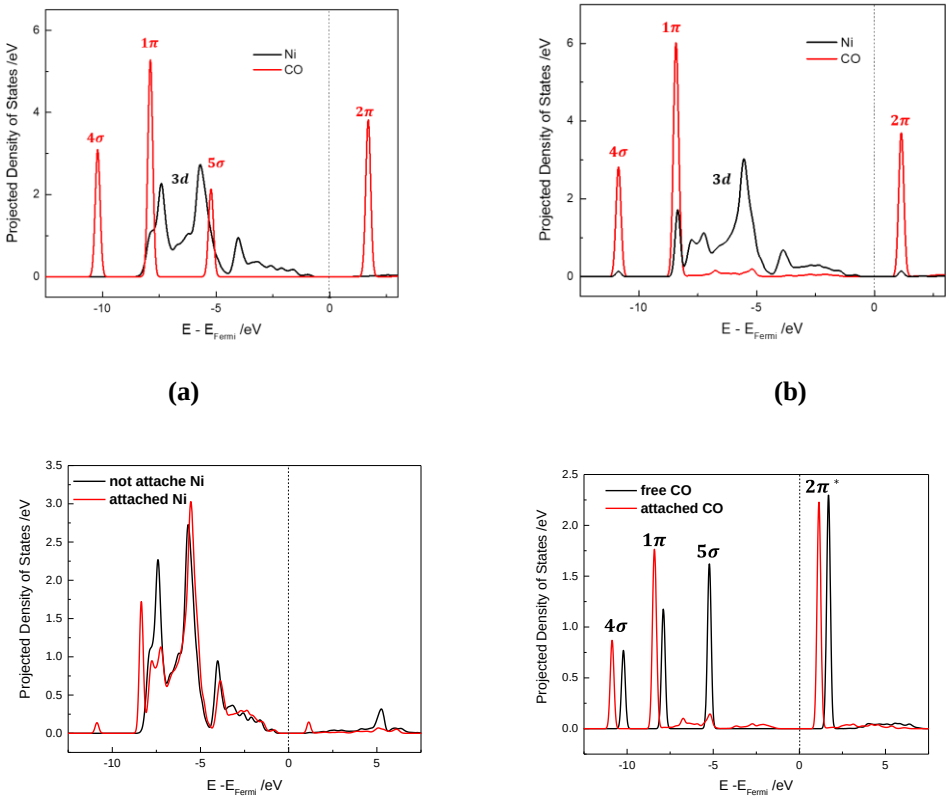

Fig. 6 Comparison between non-adsorbed system and adsorbed system (a) 3d Ni orbitals and CO molecular orbitals in non-adsorbed system (b)) 3d Ni orbitals and CO molecular orbitals in adsorbed system (c) 3d orbitals of attached Ni and non-attached Ni (d) molecular orbitals of non-attached CO and attached CO

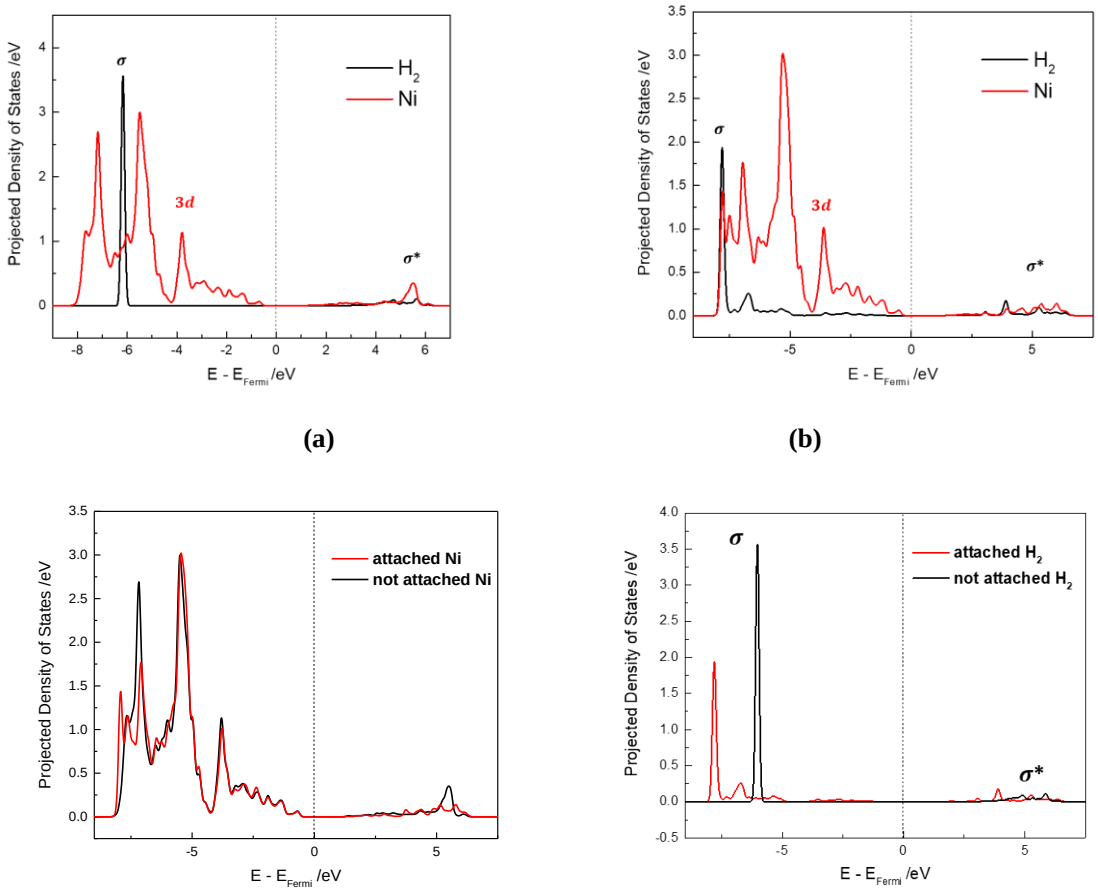

Fig. 7 Comparison between non-adsorbed system and adsorbed system (a) 3d Ni orbitals and H_2 molecular orbitals in non-adsorbed system (b)) 3d Ni orbitals and H_2 molecular orbitals in adsorbed system (c) 3d orbitals of attached Ni and non-attached Ni (d) molecular orbitals of non-attached H_2 and attached H_2

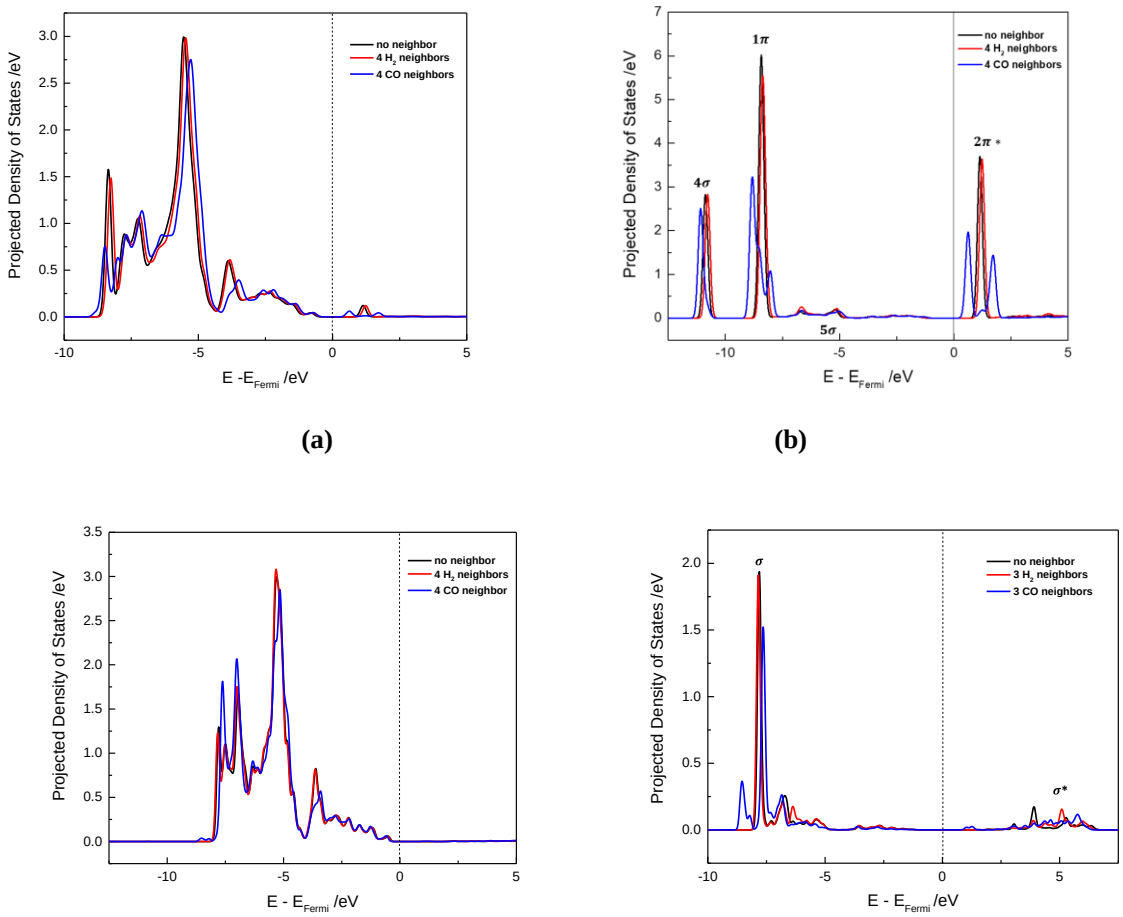

Fig. 8 neighbor effect on CO and H_2 adsorption shown in (a) 3d orbitals of Ni connected with CO (b) CO molecular orbitals (c) 3d orbitals of Ni connected with H_2 (d) H_2 molecular orbitals

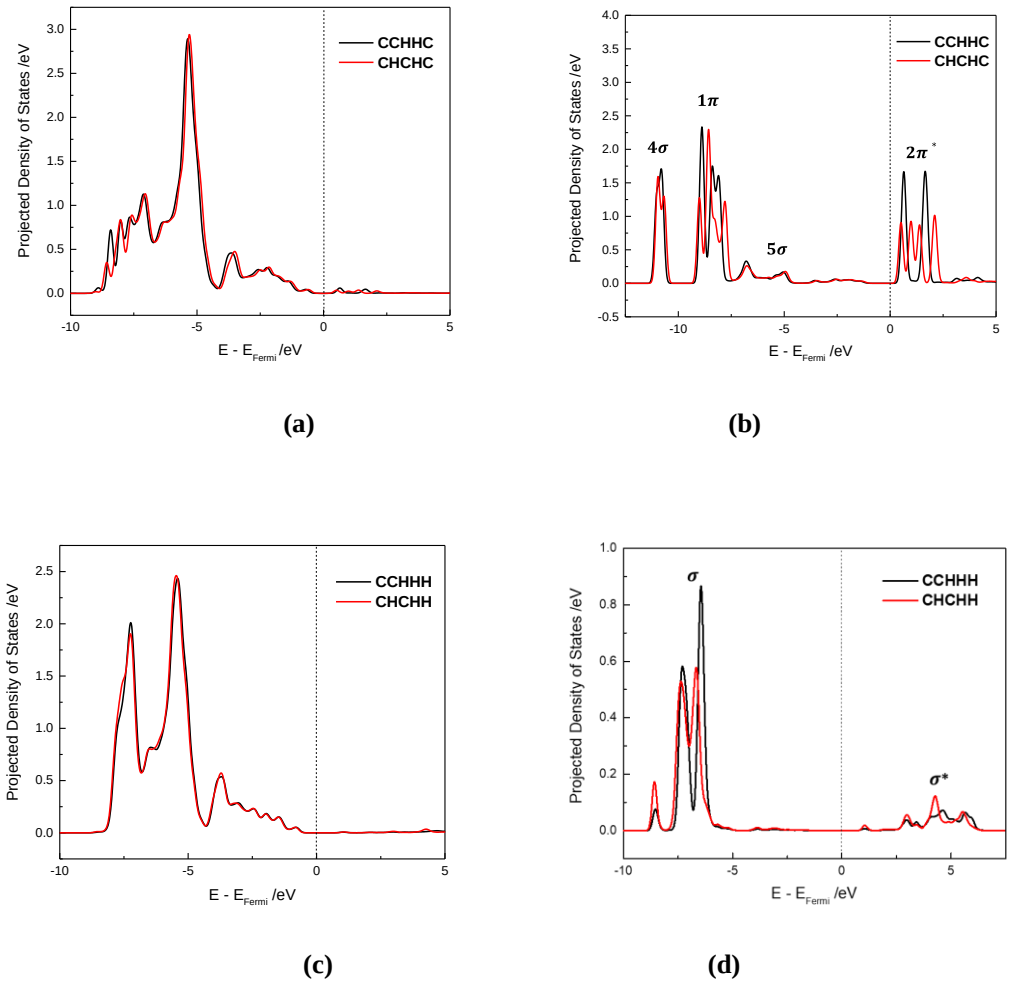

Fig. 9 symmetry effect on CO and H_2 adsorption shown in (a) 3d orbitals of Ni connected with CO (b) CO

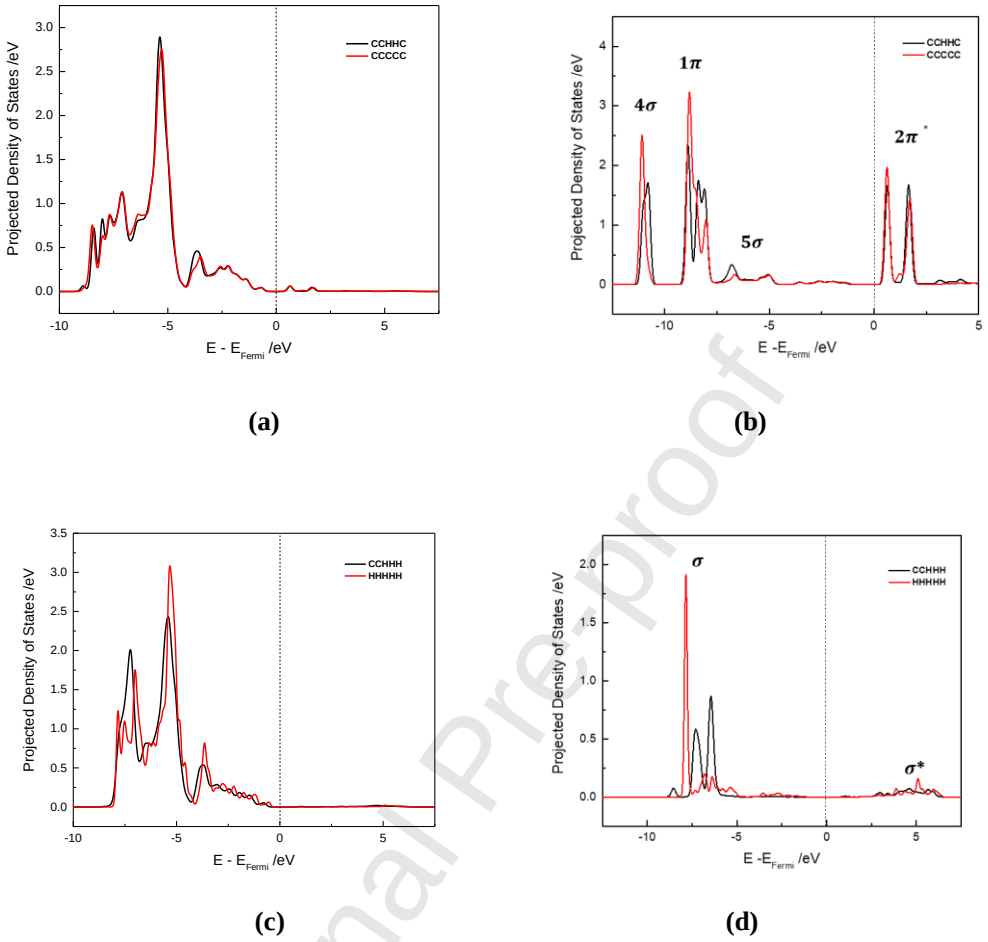

Fig. 10 hybrid effect on CO and H_2 adsorption shown in (a) 3d orbitals of Ni connected with CO (b) CO molecular orbitals (c) 3d orbitals of Ni connected with H_2 (d) H_2 molecular orbitals

Graphical abstract

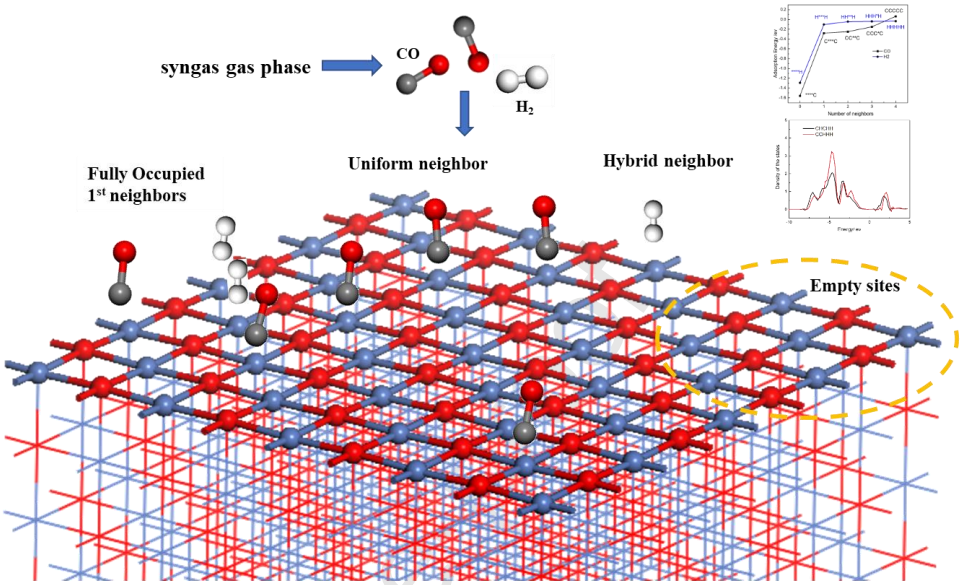

Highlights

- This study provides insights into syngas adsorption on NiO surface
- First neighbor impacts the most adsorption stability
- Hybrid effects are emphasized for the first time to predict adsorption stability
- A highly symmetric occupied neighbor geometry reduces the adsorption of syngas

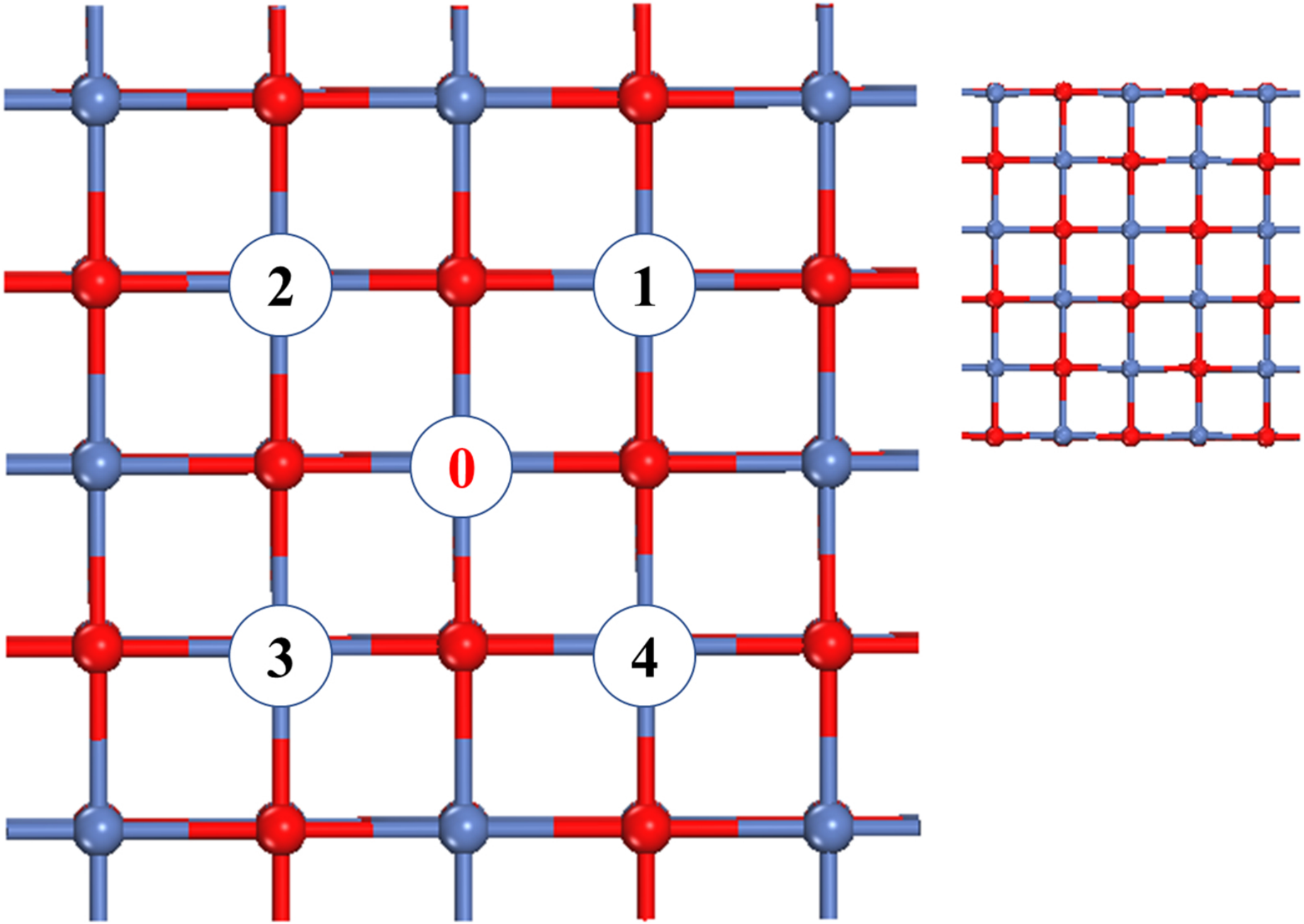

Figure 1

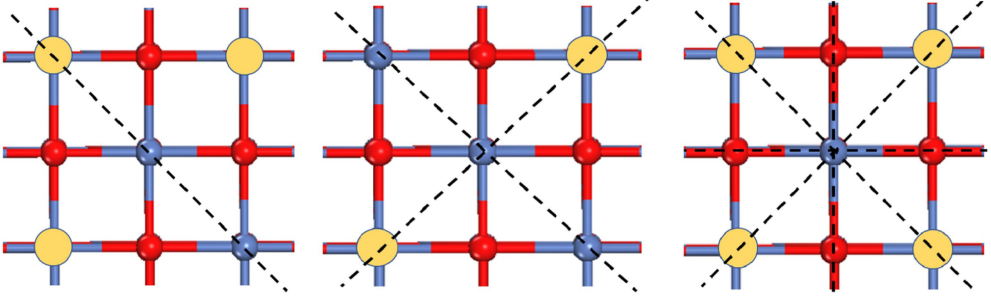

(a) **(b)** **(c)**

Figure 2

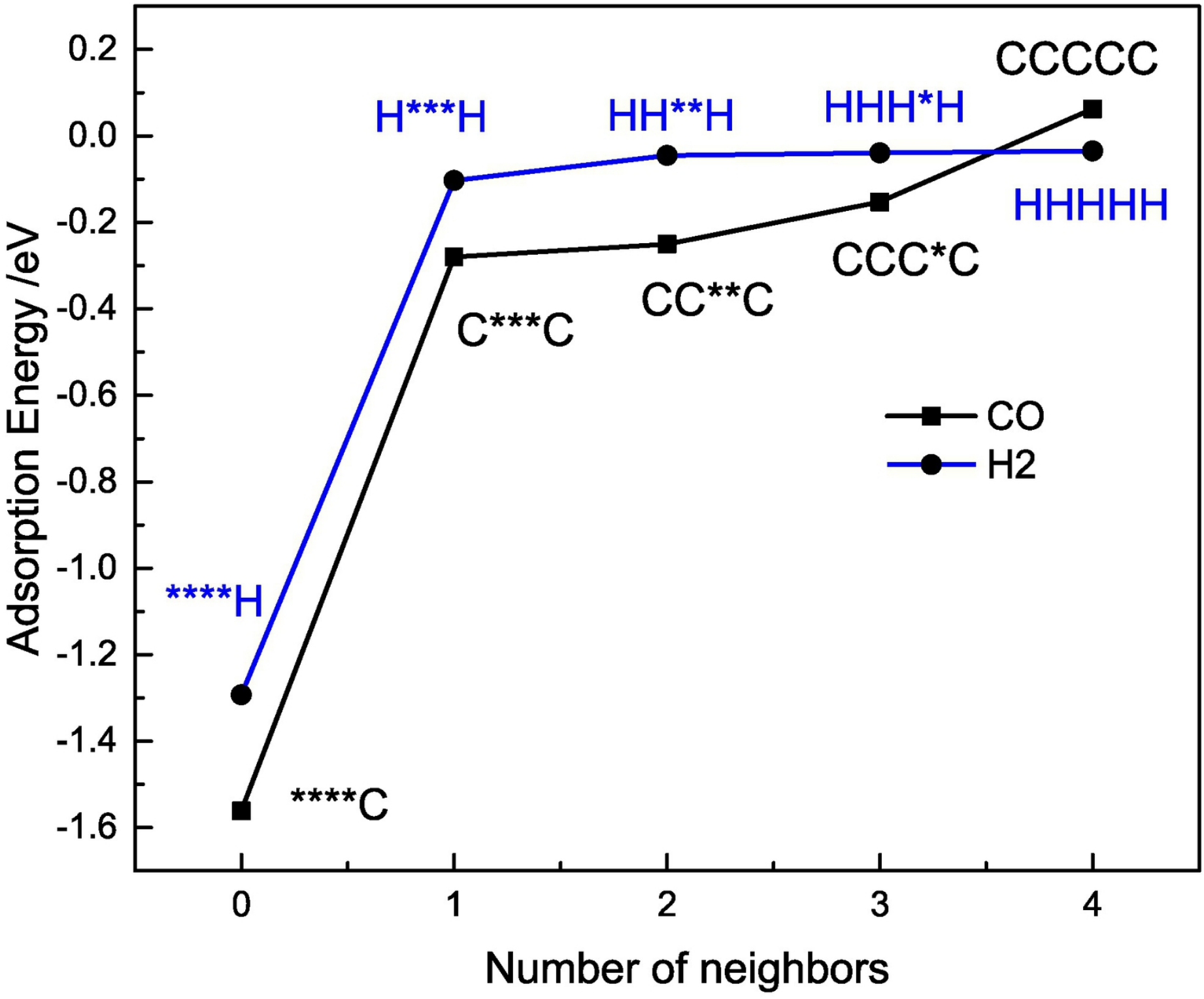
0.2
0.0
-0.2
-0.4
-0.6
-0.8
-1.0
-1.2
-1.4
-1.6
Adsorption Energy /eV
0
1
2
3
4
Number of neighbors
CCCCC
H***H
HH**H
HHH*H
HHHHH
CCC*C
CC**C
C***C
CO
H2
****H
****C

Figure 3

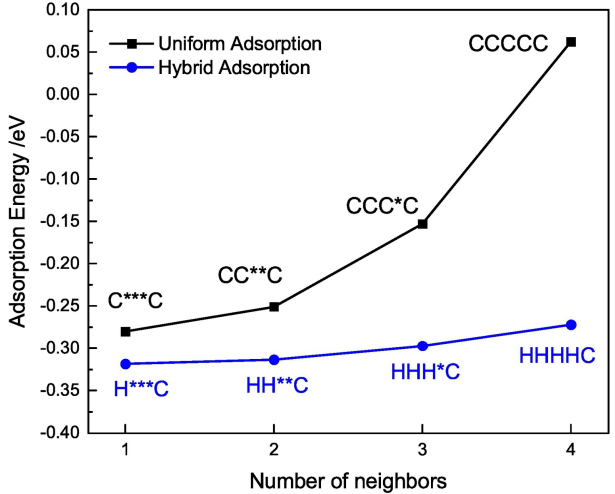
Uniform Adsorption
Hybrid Adsorption
Adsorption Energy /eV
Number of neighbors
C***C
CC**C
CCC*C
CCCCC
H***C
HH**C
HHH*C
HHHHC
0.10
0.05
0.00
-0.05
-0.10
-0.15
-0.20
-0.25
-0.30
-0.35
-0.40
1
2
3
4

(a)

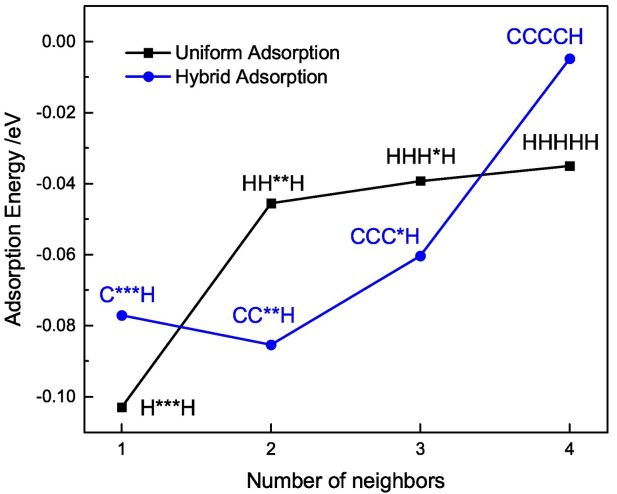
Uniform Adsorption
Hybrid Adsorption
Adsorption Energy /eV
Number of neighbors
H***H
HH**H
HHH*H
HHHHH
C***H
CC**H
CCC*H
CCCCH
0.00
-0.02
-0.04
-0.06
-0.08
-0.10
1
2
3
4

(b)

Figure 4

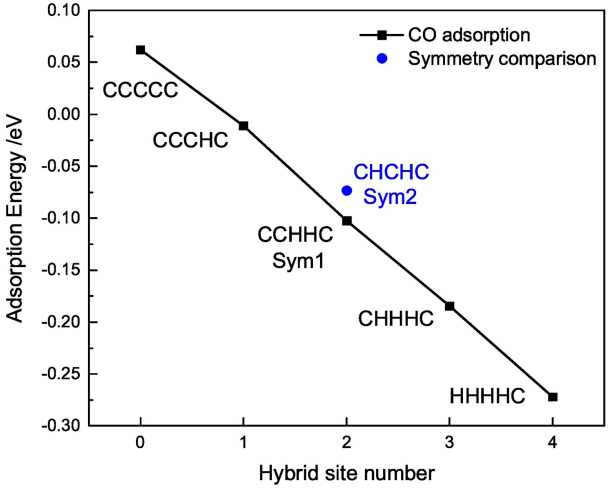
CO adsorption
Symmetry comparison
CCCCC
CCCHC
CHCHC
Sym2
CCHHC
Sym1
CHHHC
HHHHC
Adsorption Energy /eV
Hybrid site number
0.10
0.05
0.00
-0.05
-0.10
-0.15
-0.20
-0.25
-0.30
0
1
2
3
4

(a)

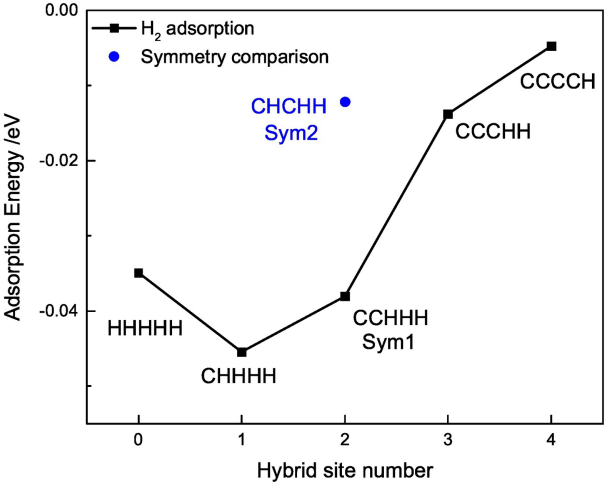
H2 adsorption
Symmetry comparison
CCCCH
CHCHH
Sym2
CCCHH
HHHHH
CHHHH
CCHHH
Sym1
Adsorption Energy /eV
Hybrid site number
0.00
-0.02
-0.04
0
1
2
3
4

(b)

Figure 5

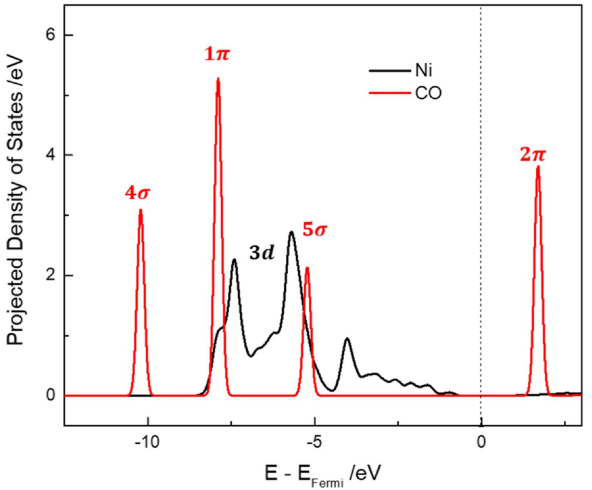

(a)

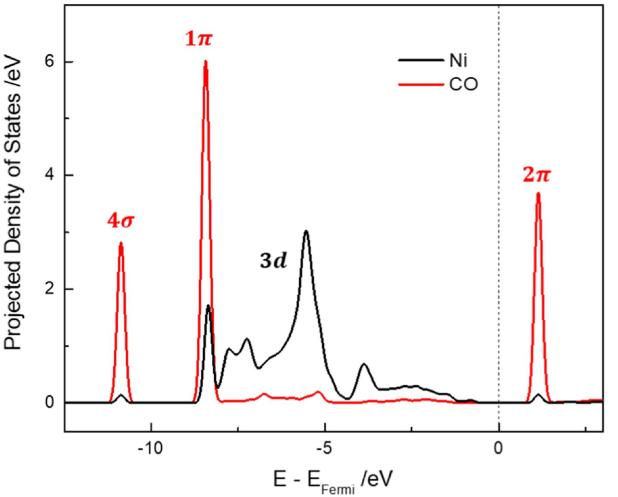

(b)

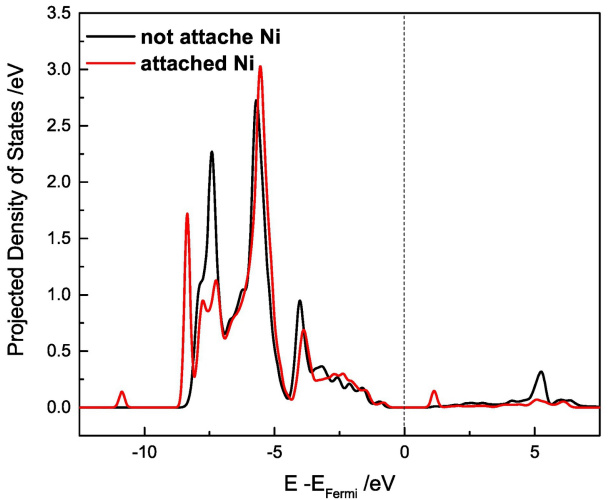

(c)

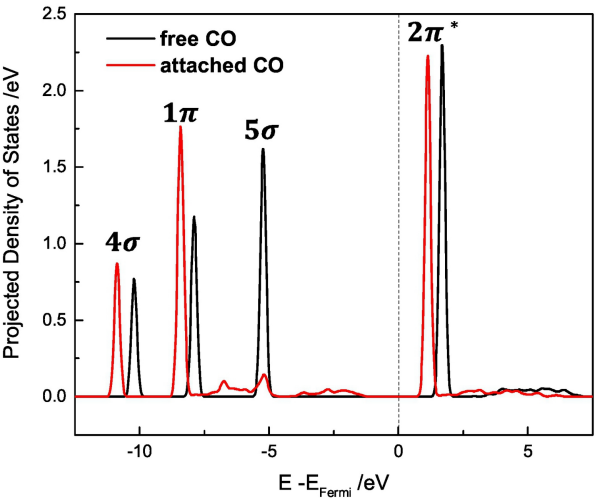

(d)

Figure 6

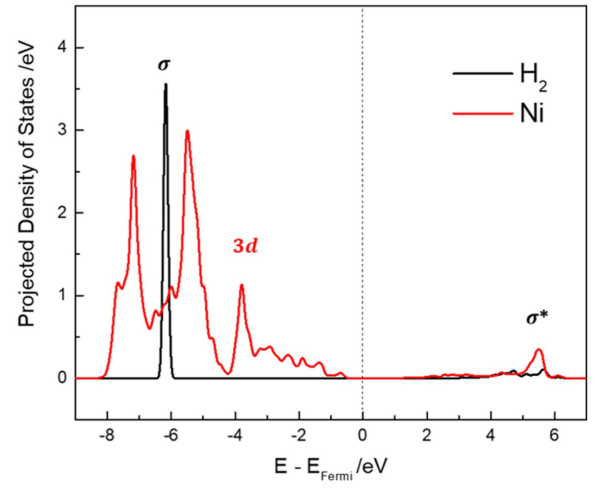

(a)

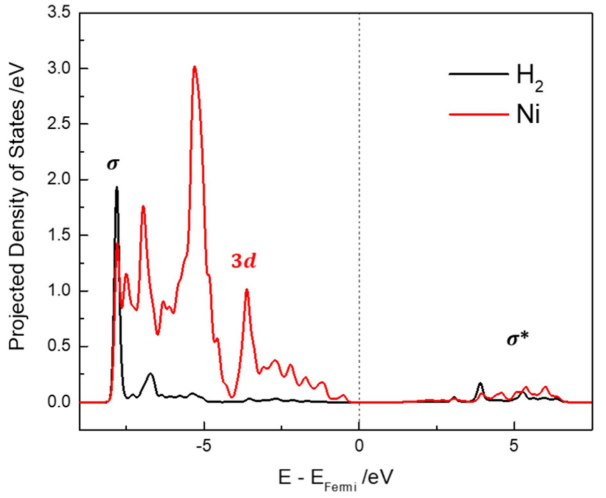

(b)

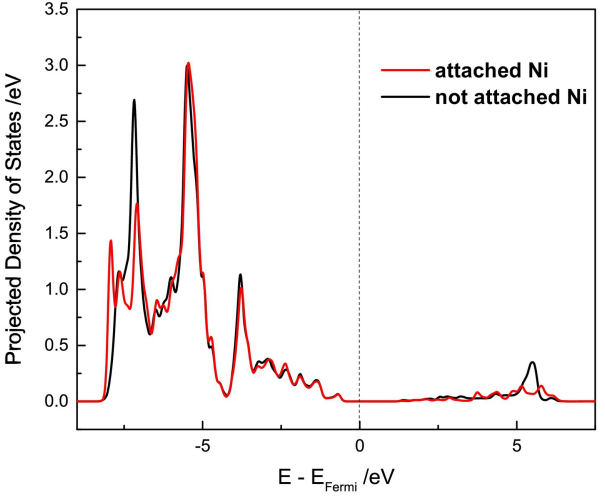

(c)

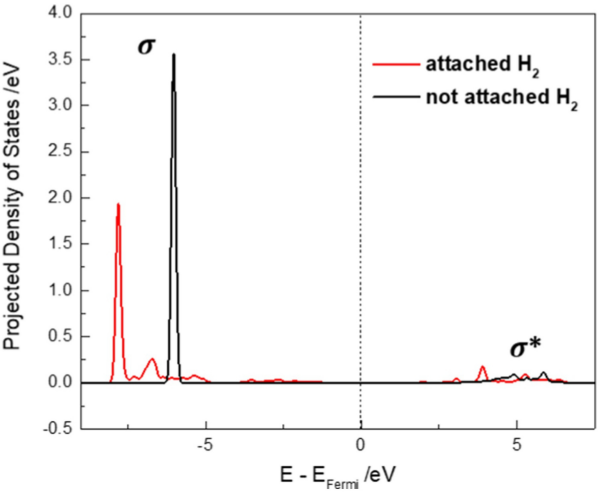

(d)

Figure 7

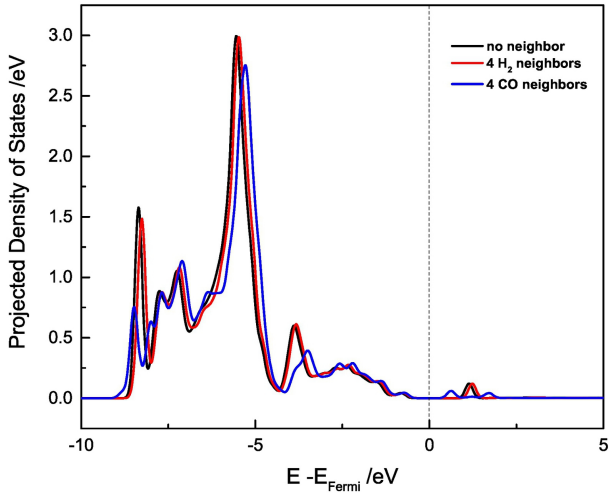

(a)

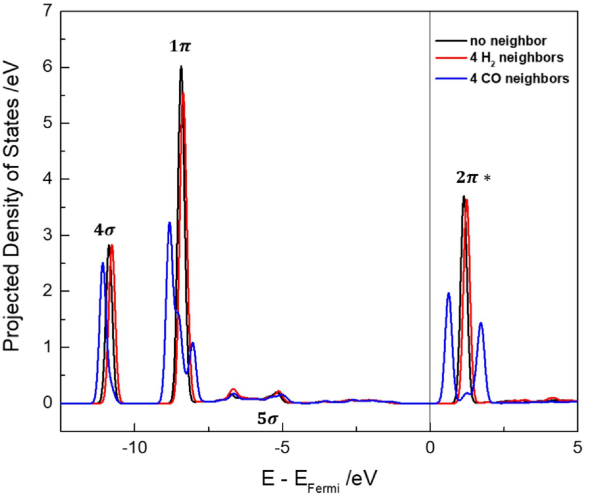

(b)

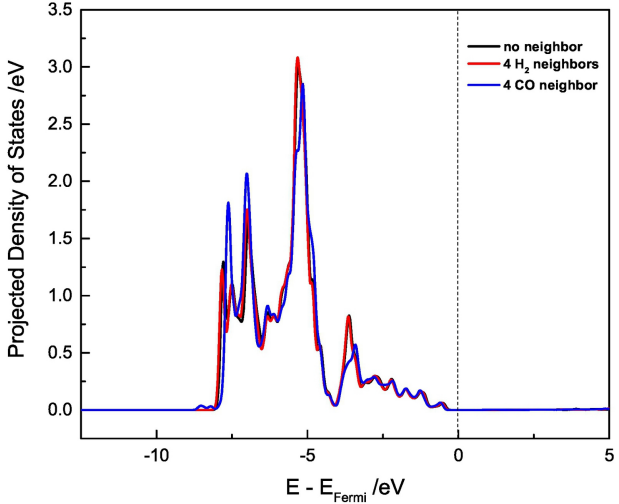

(c)

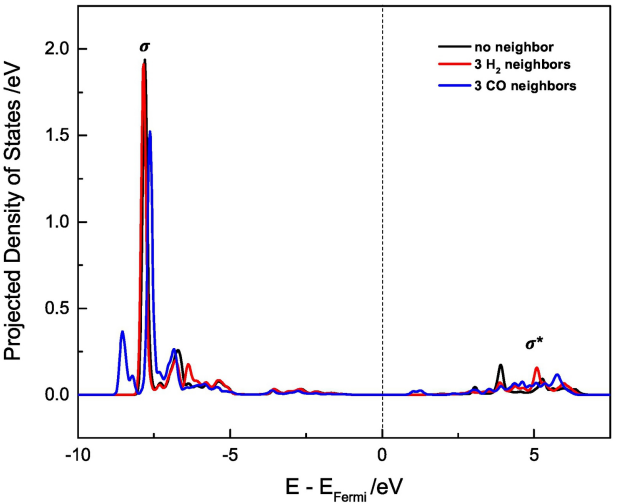

(d)

Figure 8

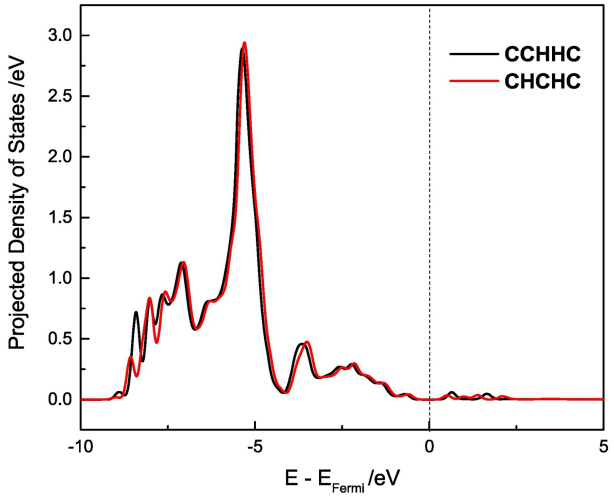

(a)

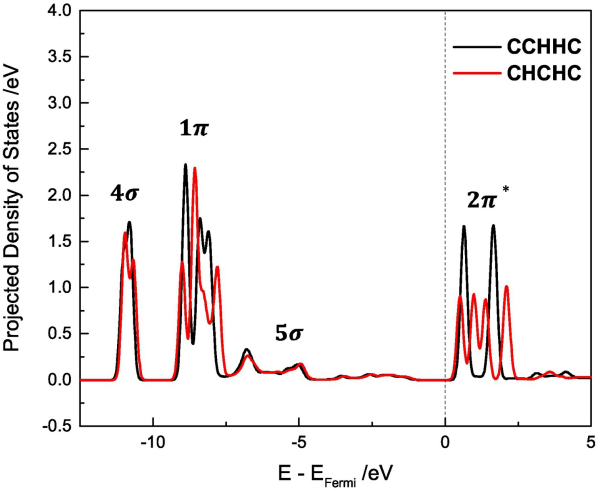

(b)

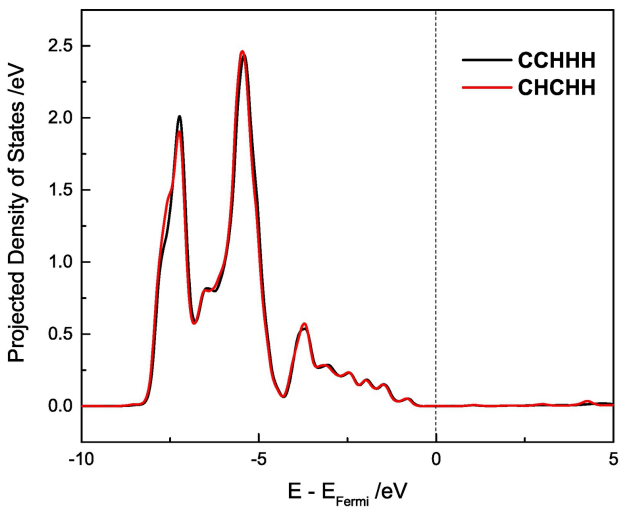

(c)

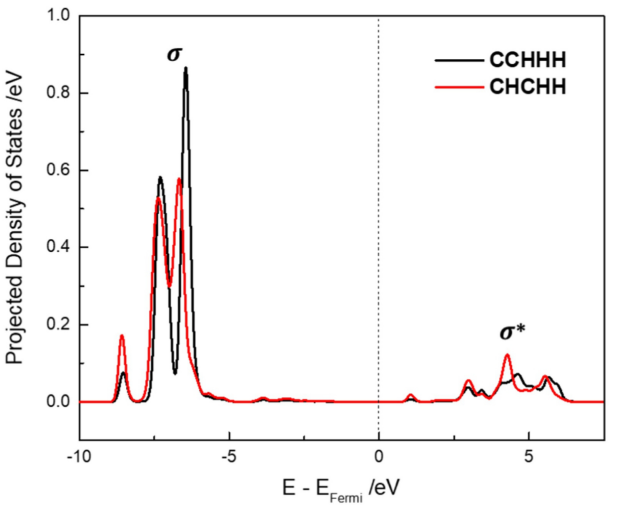

(d)

Figure 9

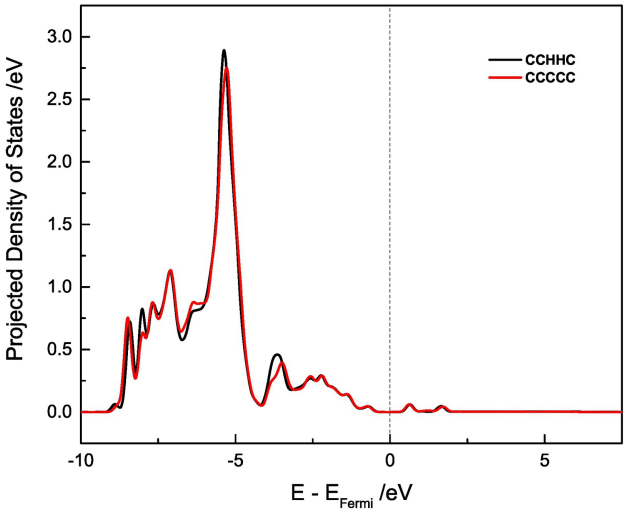

(a)

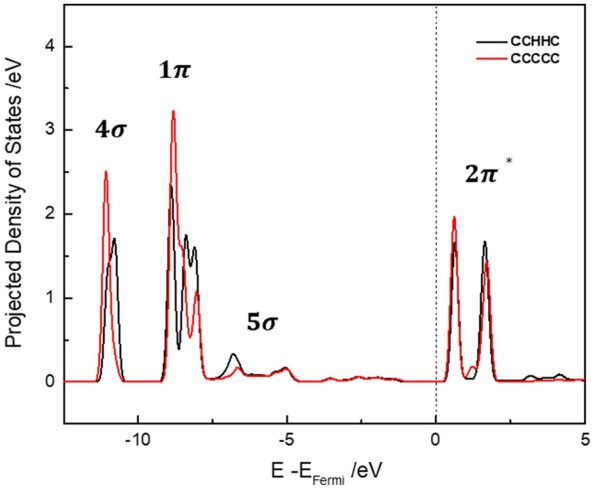

(b)

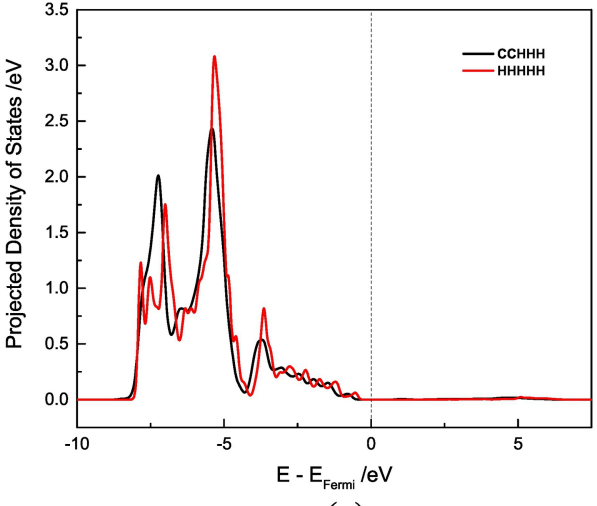

(c)

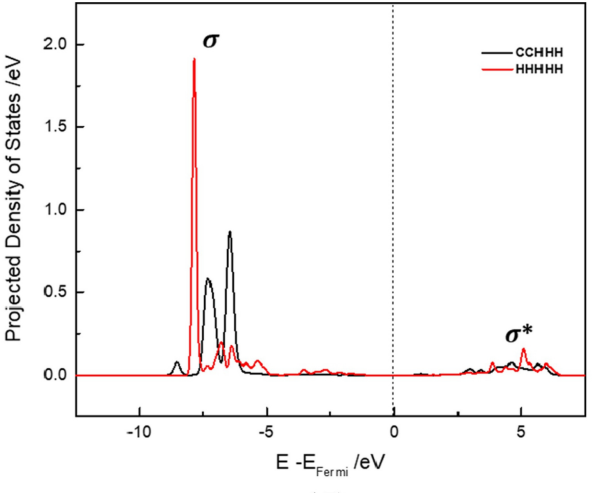

(d)

Figure 10